SECOND ORDER GUIDED WAVE PROPAGATION IN LAYERED PLATES

A. Pysarenko[1]
[1]*Odessa State Academy of Civil Engineering and Architecture*

Abstract: This paper presents a comprehensive theoretical study of the mechanism of generation of combined harmonics of the second and third orders, which arise as a result of collinear cross-interaction of two primary directional Lamb waves in thin layered plates. The developed and implemented procedure for measuring combined harmonics at certain mixing frequencies allowed us to verify and confirm previously formulated theoretical predictions. In particular, it was established that for effective generation of combined harmonics, simultaneous fulfillment of two key conditions is necessary: the synchronism condition, which ensures phase coincidence of the interacting waves, and the symmetry condition, which determines the nature of the spatial properties of the formed harmonics. The results of numerical analysis showed that the frequency mixing response in the sample is due exclusively to the collinear cross-interaction between two primary Lamb waves propagating in the same direction. A cumulative effect of the increase in the amplitude of combined harmonics with the propagation distance in the mixing zone was revealed, which indicates the strengthening of nonlinear effects with an increase in the length of wave interaction. This effect is fully consistent with theoretical predictions and confirms the physical nature of the process of generating combined harmonics. Particular attention is paid to a detailed analysis of the symmetrical properties of second-order harmonics. It was found that the combined harmonic mode of the second order, which is generated at the total frequency, should have an antisymmetric character. This is due to the specificity of the cross-interaction between the A1 and S0 modes, which have different symmetrical properties. The lack of the appearance of a symmetrical mode of the combined harmonic of the second order is explained by the impossibility of simultaneously fulfilling the conditions of synchronism and symmetry, which imposes strict restrictions on the possible generation modes. The proposed theoretical model allows us to describe the frequency response of mixing, the conditions of internal resonance, as well as the features of symmetry that determine the appearance of combined harmonics at certain mixing frequencies. The model takes into account the physical process of generation of combined second- and third-order harmonics caused by the collinear cross-interaction of two primary Lamb waves propagating in the sample. This approach allows us to gain an understanding of the mechanism of nonlinear wave interaction in layered plates and contributes to the development of nonlinear acoustics methods. The results obtained are of great importance for practical application in the field of materials diagnostics, as they allow us to more accurately determine the properties of materials and detect defects by analyzing nonlinear effects in Lamb waves.

Keywords: combined harmonics, Lamb waves, collinear cross-interaction, synchronism condition, internal resonance.

ПОШИРЕННЯ КЕРОВАНИХ ХВИЛЬ ДРУГОГО ПОРЯДКУ У ШАРУВАТИХ ПЛАСТИНАХ

Писаренко О. М. [1]
[1]*Одеська державна академія будівництва та архітектури*

Анотація: У роботі представлено комплексне теоретичне дослідження механізму генерації комбінованих гармонік другого та третього порядків, що виникають у результаті колінеарної перекрестної взаємодії двох первинних керованих хвиль Лемба в тонких шаруватих пластинах. Розроблена та реалізована процедура вимірювання комбінованих

гармонік на визначених частотах змішування дозволила перевірити та підтвердити раніше сформульовані теоретичні передбачення. Зокрема, встановлено, що для ефективної генерації комбінованих гармонік необхідне одночасне виконання двох ключових умов: умови синхронизму, яка забезпечує фазове співпадіння взаємодіючих хвиль, та умови симетрії, що визначає характер просторових властивостей утворених гармонік. Результати чисельного аналізу показали, що відгук змішування частот у зразку обумовлений виключно колінеарним перекрестним взаємодією між двома первинними хвилями Лемба, які поширюються в одному напрямку. Виявлено кумулятивний ефект наростання амплітуди комбінованих гармонік із відстанню поширення у зоні змішування, що свідчить про посилення нелінійних ефектів при збільшенні довжини взаємодії хвиль. Цей ефект повністю узгоджується з теоретичними прогнозами і підтверджує фізичну природу процесу генерації комбінованих гармонік. Особливу увагу приділено детальному аналізу симетричних властивостей гармонік другого порядку. З'ясовано, що комбінована гармонічна мода другого порядку, яка генерується на сумарній частоті, повинна мати антисиметричний характер. Це обумовлено специфікою перекрестного взаємодії між модами A1 та S0, які мають різні симетричні властивості. Відсутність появи симетричного режиму комбінованої гармоніки другого порядку пояснюється неможливістю одночасного виконання умов синхронизму та симетрії, що накладає суворі обмеження на можливі режими генерації. Запропонована теоретична модель дозволяє описати частотний відгук змішування, умови внутрішнього резонансу, а також особливості симетрії, які визначають появу комбінованих гармонік на визначених частотах змішування. Модель враховує фізичний процес генерації комбінованих гармонік другого і третього порядків, викликаних колінеарним перекрестним взаємодією двох первинних хвиль Лемба, що поширюються в зразку. Такий підхід дає змогу отримати розуміння механізму нелінійної взаємодії хвиль у шаруватих пластинах і сприяє розвитку методів нелінійної акустики. Отримані результати мають важливе значення для практичного застосування у сфері діагностики матеріалів, оскільки дозволяють більш точно визначати властивості матеріалів та виявляти дефекти шляхом аналізу нелінійних ефектів у хвилях Лемба.

Ключові слова: комбіновані гармоніки, хвилі Лемба, колінеарна перекрестна взаємодія, умова синхронизму, внутрішній резонанс.

1 INTRODUCTION

The linear feature of ultrasonic wave propagation, while widely utilized in nondestructive evaluation (NDE), is not sufficiently sensitive to detect microscopic degradation or micro-damage within materials. This limitation arises because linear ultrasonic techniques primarily respond to changes in bulk material properties, such as velocity and attenuation, which often do not exhibit significant variation until damage has progressed to a more advanced stage. In contrast, even very small imperfections or microstructural changes–such as dislocations, micro-cracks, or voids–can induce pronounced nonlinear elastic behavior in materials. These nonlinearities can manifest as higher-order harmonic generation or modulation effects, which are orders of magnitude larger than the intrinsic nonlinearity observed in intact, undamaged materials. Consequently, the nonlinear ultrasonic response has emerged as a highly promising and sensitive approach for the early detection and characterization of material degradation and micro-damage.

Over the past two decades, extensive research has demonstrated that nonlinear ultrasonic methods can reveal subtle changes in material microstructure that remain undetectable by conventional linear ultrasonic techniques. The sensitivity of nonlinear ultrasonic measurements to microstructural defects stems from their ability to probe the material's nonlinear elastic constants, which are directly influenced by damage mechanisms at the microscopic scale. This enhanced sensitivity enables the detection of incipient damage, fatigue, and other forms of degradation well before macroscopic failure occurs, thereby providing critical information for predictive maintenance and structural health monitoring.

Among the various nonlinear ultrasonic techniques, the use of Lamb waves has gained significant attention due to their unique propagation characteristics in plate-like structures. Lamb waves are guided elastic waves that travel along thin plates and exhibit multiple modes with dispersive behavior, making them highly versatile for interrogating complex geometries and layered materials. The nonlinear ultrasonic Lamb wave approach combines the inherent advantages of Lamb wave inspection–such as long-range propagation and mode selectivity–with the high sensitivity of nonlinear acoustic measurements. This synergy offers a powerful tool for evaluating material nonlinearity and detecting micro-damage in engineering components like aircraft skins, pipelines, and composite laminates.

To date, theoretical investigations into the nonlinear behavior of ultrasonic Lamb waves in isotropic plates have employed perturbation approximations and modal expansion analyses to model higher-harmonic generation phenomena. These studies provide fundamental insights into the mechanisms by which nonlinear Lamb waves interact with material imperfections and how higher harmonics evolve during wave propagation. Understanding these nonlinear interactions is essential for optimizing experimental setups, interpreting measurement data, and developing robust diagnostic criteria for damage assessment. As research progresses, the nonlinear ultrasonic Lamb wave approach is poised to become an integral part of advanced NDE methodologies, offering unprecedented sensitivity and reliability in the evaluation of material integrity.

2 ANALYSIS OF LITERARY DATA AND RESOLVING THE PROBLEM

The generation of higher harmonics and the possibility of symmetric or antisymmetric Lamb waves at higher harmonics have in layered structures been described in numerous studies [1, 2]. This problem was addressed using displacement gradient shaping in modal decomposition [3, 4]. As shown in these studies, the second harmonic of the propagation of the primary (fundamental) Lamb wave exhibits a cumulative effect under conditions of phase velocity matching and non-zero power transfer from the primary to the second

harmonic. Experimental studies were carried out to confirm the theoretical predictions, and the results showed that Lamb waves can grow with propagation distance [5, 6].

However, most of the previous studies focused on the generation of higher harmonics of primary Lamb waves with a single frequency. In contrast, there are few studies that discuss the frequency mixing response caused by the collinear interaction of two primary Lamb waves with different frequencies [7, 8]. The interaction of two primary waves with fixed frequencies in nonlinear materials can generate combined harmonics with different frequencies [9, 10]. The possibility of using collinear mixing of body waves to measure acoustic nonlinearity has been considered as a model approach to solving the problem [11, 12]. In addition, the identification of local plastic damage using the nonlinear response of scanning collinear mixing of body waves has been investigated [13, 14]. It has been shown that non collinear mixing of body waves can be used to assess ductility and fatigue, respectively [15, 16]. Nonlinear mixing of ultrasonic waves can be used to assess the physical aging of thermoplastics and the curing of epoxy resins [17, 18]. Necessary and sufficient conditions for the generation of resonant harmonic modes by mixing two propagating waves in solids with quadratic elastic nonlinearity were also discussed [19, 20]. The frequency response of mixing offers some unique advantages over nonlinear ultrasonic technology based on higher harmonic generation, such as frequency selectivity, which allows one to intentionally avoid receiving unexpected harmonic components induced by instrumentation systems. Furthermore, the spatial selectivity of scanning wave mixing can be easily exploited to locate the damage region in a material.

In this paper, a theoretical model is presented to describe the frequency mixing response caused by the collinear cross-talk of two primary Lamb waves, as well as the physical process of generating the second- and third-order combined harmonics. Based on this theoretical framework, the internal resonance conditions, including the synchronism and symmetry features for the generation of the second- and third-order combined harmonics by two primary Lamb waves, will be analyzed. In addition, the possibility of predicting the existence of the second- and third-order combined harmonics at certain mixing frequencies needs to be separately considered. The possibility of generating the second- and third-order combined harmonics caused by the collinear cross-talk of two primary Lamb waves also needs to be substantiated.

3 PURPOSE AND TASKS OF THE STADY

The equation of motion for elastic wave propagation in an isotropic, homogeneous, nonlinear elastic material is given by

$$\rho_0 \frac{\partial^2 v}{\partial t^2} + \mu \nabla (\nabla v) - (\lambda + 2\mu) \nabla (\nabla \mathrm{v}) = Y(v),$$

where v is the mechanical displacement; λ and μ are the second-order elastic constants; ρ_0 is the initial mass density of material.

Functional dependency $Y = Y(v)$ nonlinear term with respect to v. The perturbation approximation can be used to solve nonlinear wave equations. The solution for v can be approximated as the sum of the primary (fundamental or first-order) wave $v^{(1)}$, the second-order wave $v^{(2)}$, and the third-order wave $v^{(3)}$, i.e.

$$v = v^1 + v^2 + v^3.$$

These equations can be decomposed into the following three second order guided wave equations:

$$\rho_0 \frac{\partial^2 v^{(1)}}{\partial t^2} + \mu \nabla^2 v^{(1)} - (\lambda + \mu) \nabla (\nabla \cdot v^{(1)}) = 0,$$

$$\rho_0 \frac{\partial^2 v^{(2)}}{\partial t^2} + \mu \nabla^2 v^{(2)} - (\lambda + \mu) \nabla (\nabla \cdot v^{(2)}) = Y^{(2)},$$

$$\rho_0 \frac{\partial^2 v^{(3)}}{\partial t^2} + \mu \nabla^2 v^{(3)} - (\lambda + \mu) \nabla (\nabla \cdot v^{(3)}) = Y^{(3)},$$

where $Y^{(2)} = Y[v^{(1)}]$ and $Y^{(3)} = Y[v^{(1)}, v^{(2)}]$ are the second and third-order nonlinear terms, respectively, which can be obtained from $Y = Y(v)$ just using $v^{(1)} = v^{(2)} + v^{(3)}$ instead of v.

In this paper, the calculation method has as a working object a reference configuration for the analysis of guided Lamb wave propagation in a single elastic plate, where the material is assumed to be homogeneous, without dispersion and attenuation of waves, with weak elastic nonlinearity. Before performing the calculations, it was assumed that in the plate material Lamb waves propagate along the axis of a fixed p-axis of symmetry oz, and the corresponding mechanical displacements are considered only in the perpendicular plane yz.

Based on this consideration, the formal solutions of two primary Lamb waves with different frequencies propagating along the oz axis are given by $v_a = v_a(y) \exp(j(k_a z - \omega_a t))$ and $v_b = v_b(y) \exp(j(k_b z - \omega_b t))$, respectively, which satisfy the stress-free boundary conditions. Here, $v_a(y)$ and $v_b(y)$ are the field functions of the two primary Lamb waves with angular frequencies ω_a and ω_b and wave numbers k_a and k_b, respectively.

Clearly, $v_a + v_b$ corresponds the primary wave $v^{(1)}$. The second order self- and cross-interactions of the two primary waves v_a and v_b can generate the second-order wave $v^{(2)}$, while the third-order self- and cross-interactions of v_a and v_b generate the third-order wave $v^{(3)}$. Considering that the two primary Lamb waves v_a and v_b propagate in the same direction, all the self- and cross-interactions associated with v_a and v_b are collinear.

Considering all possible self- and cross-interactions of the two primary Lamb waves v_a and v_b propagating in the plate, the nonlinear terms $Y^{(2)}$ and $Y^{(3)}$ can be formally decomposed as

$$Y^{(2)} = y^{(2a)} exp\left[2j(k_a z - \omega_a t)\right] + y^{(2b)} exp\left[2j(k_b z - \omega_b t)\right] +$$
$$+ y^{(a \pm b)} exp\left\{j\left[(k_a \pm k_b)z - (\omega_a \pm \omega_b)t\right]\right\},$$

and

$$Y^{(3)} = y^{(3a)} exp\left[3j(k_a z - \omega_a t)\right] + y^{(3b)} exp\left[3j(k_b z - \omega_b t)\right] +$$
$$+ y^{(2a \pm b)} exp\left\{j\left[(2k_a \pm k_b)z - (2\omega_a \pm \omega_b)t\right]\right\} +$$
$$+ y^{(a \pm 2b)} exp\left\{j\left[(k_a \pm 2k_b)z - (\omega_a \pm 2\omega_b)t\right]\right\}.$$

Here, $y^{(2a)}, y^{(2b)}, y^{(3a)}$, and $y^{(3b)}$ are the second- and third order driving forces induced by the self-interactions of primary waves v_a and v_b, respectively, while $y^{(a \pm b)}, y^{(2a \pm b)}$, and $y^{(a \pm 2b)}$ are induced by the second- and third-order cross-interactions of v_a and v_b.

For v_a and v_b propagating in the plate, in addition to the existence of $Y^{(2)} = Y\left[v^{(1)}\right]$ and $Y^{(2)} = Y\left[v^{(1)}, v^{(2)}\right]$ inside the solid plate, second-and third-order traction stress tensors $S^{(2)} \cdot n_y$ and $S^{(3)} \cdot n_y$ exist at the two surfaces of the plate $(\pm h)$, which can be formally expressed as

$$S^{(2)} \cdot n_x = s^{(2a)} \cdot n_x exp\left[2j\left(k_a z - \omega_a t\right)\right] + s^{(2b)} \cdot n_x exp\left[2j\left(k_b z - \omega_b t\right)\right] +$$
$$+ s^{(a\pm b)} \cdot n_x exp\left\{j\left[\left(k_a \pm k_b\right)z - \left(\omega_a \pm \omega_b\right)t\right]\right\},$$

and

$$S^{(3)} \cdot n_x = s^{(3a)} \cdot n_x exp\left[3j\left(k_a z - \omega_a t\right)\right] + s^{(3b)} \cdot n_x exp\left[3j\left(k_b z - \omega_b t\right)\right] +$$
$$+ s^{(2a\pm b)} \cdot n_x exp\left\{j\left[\left(2k_a \pm k_b\right)z - \left(2\omega_a \pm \omega_b\right)t\right]\right\} +$$
$$+ s^{(a\pm 2b)} \cdot n_x exp\left\{j\left[\left(k_a \pm 2k_b\right)z - \left(\omega_a \pm 2\omega_b\right)t\right]\right\}.$$

In these equations n_x and n_y are the unit vector along the oy and oz axes, respectively, and $S^{(2)}$ and $S^{(3)}$ correspond to the quadric and cubic terms, respectively, in the expression of the first Piola–Kirchhoff stress tensor. Specifically, $s^{(2a)} \cdot n_x$, $s^{(2b)} \cdot n_x$, $s^{(3a)} \cdot n_x$, and $s^{(3b)} \cdot n_x$ are the second- and third order traction stress tensors at the surfaces induced by the self-interactions of primary wave v_a and v_b, respectively, while $s^{(a\pm b)} \cdot n_x$, $s^{(2a\pm b)} \cdot n_x$, and $+ s^{(a\pm 2b)} \cdot n_x$ are induced by the second- and third- order cross-interactions of v_a and v_b.The expressions for $s^{(a\pm b)}$, $s^{(2a\pm b)}$, and $s^{(a\pm 2b)}$ are extremely lengthy for any modes v_a and v_b.

According to the modal-expansion approach for wave guide excitation, the bulk driving forces $Y^{(2)}, Y^{(3)}$ and the surface stress tensors $S^{(2)} \cdot n_x$ and $S^{(3)} \cdot n_x$ can be thought of as a bulk source and a surface source, respectively, and their function is to generate a series of second and third-order Lamb waves propagating in the stress-free plate. In the present investigation, we focus on the combined harmonic modes generated at the mixing frequency. Thus, only the nonlinear terms $y^{(a\pm b)}$ and $s^{(a\pm b)} \cdot n_x$ are taken into account for generating second-order combined harmonics at the mixing frequency $\omega^{(2)} = \omega_a \pm \omega_b$, where as the self-interaction terms of the two primary waves are neglected for the analysis of the second-order nonlinear wave problem. Based on this consideration, we focus on analyzing the combined harmonic wave $v^{(2)}$ at $\omega^{(2)} = \omega_a \pm \omega_b$, which is generated by $y^{(a\pm b)}$ and $s^{(a\pm b)} \cdot n_x$.

We construct the solution of the second-order combined harmonic $v^2 = v^{\left(\omega_a \pm \omega_b\right)}$ via a modal-expansion analysis. The field caused by mixing the two primary Lamb waves (i.e., v_a and v_b) can be written as a linear combination of a series of Lamb waves at the mixing frequency $\omega^{(2)} = \omega_a \pm \omega_b$

$$v^{(2)} = \sum_m A_m\left(z\right) v_m^{\left(\omega_a \pm \omega_b\right)}\left(y\right) exp\left[-j\left(\omega_a \pm \omega_b\right)t\right],$$

where $v_m^{\left(\omega_a \pm \omega_b\right)}$ is the field function of the mth Lamb wave at the mixing frequency $\omega^{(2)}$ with wave number $k_m^{(2)}$, and $A_m\left(z\right)$ is the corresponding expansion coefficient. Similar to

the analysis of second-harmonic generation by the primary Lamb wave, the equation governin $A_m(z)$ is given by

$$4Y_{mm}\left[\frac{d}{dz} - jk_m^{(2)}\right]A_m(z) = \left[y_{s,(m)}^{(2)} + y_{b,(m)}^{(2)}\right]exp\left[j\left(k_a \pm k_b\right)z\right],$$

where

$$y_{b,(m)}^{(2)} = \int_{-h}^{h} j\left(\omega_a \pm \omega_b\right)\left[v_m^{(\omega_a \pm \omega_b)}\left(x\right)\right]\cdot y^{(a\pm b)}dy$$

$$y_{s,(m)}^{(2)} = j(\omega_a \pm \omega_b)[v_m^{(\omega_a \pm \omega_b)}(x)]\cdot y^{(a\pm b)}\cdot n_x\big|_{(-h)}^{h}.$$

are the excitation functions due to the bulk driving force $y^{(a\pm b)}$.

The quantity Y_{mm} is the average power flow per unit width along the ox axis for the mth Lamb wave at the mixing frequency $\omega^{(2)} = \omega_a \pm \omega_b$. The formal expression of Y_{mm} is

$$Y_{mm} = Re\frac{1}{2}\int_{-h}^{h}\left[-j\left(\omega_a \pm \omega_b\right)\right]\begin{bmatrix} n_x v_m^{(\omega_a \pm \omega_b)}\left(x\right)T_{(m)xz}\left(x\right) \\ n_z v_m^{(\omega_a \pm \omega_b)}\left(x\right)T_{(m)zz}\left(x\right) \end{bmatrix}dy,$$

where $T_{(m)xz}(x) = n_x T_m n_z$, $T_{(m)zz}(x) = n_z T_m n_z$, T_m is the stress tensor related to $v_m^{(\omega_a \pm \omega_b)}(x)$.

Fixed coefficient $A_m(z)$ can be formally expressed as

$$A_m(z) = \frac{\left[y_{s(m)}^{(2)} + y_{b(m)}^{(2)}\right]}{4Y_{mm}}\frac{sin(\Delta_m z)}{\Delta_m}exp\left[j\left(k_m^2 + \Delta_m\right)z\right],$$

where

$$\Delta_m = \frac{\left[\left(k_a \pm k_b\right) - k_m^{(2)}\right]}{2}.$$

Next, we analyzed the effect of synchronism (also called phase matching between the primary wave and the mth combined harmonic mode at the frequency $\omega^{(2)} = \omega_a \pm \omega_b$. The magnitude of the mth combined harmonic mode is closely related to Δ_m. Thus, the effect of synchronism on the generation of the mth combined harmonic mode can be revealed directly by the dependence of $A_m(z)$ on the factor $sin(\Delta_m z)/\Delta_m$. For the synchronism condition [i.e., $k_m^2 = k_a \pm k_b$] at $\omega^{(2)} = \omega_a \pm \omega_b$, the factor $sin(\Delta_m z)/\Delta_m = z$, and the magnitude of the mth combined harmonic mode increases linearly with z provided $y_{s(m)}^{(2)} + y_{b(m)}^{(2)} \neq 0$. For $k_m^2 \neq k_a \pm k_b$ and $y_{s(m)}^{(2)} + y_{b(m)}^{(2)} \neq 0$, the magnitude of $\left|A_m(z)\right|\cdot\left|sin(\Delta_m z)\right|$ remains bounded and oscillates with a spatial periodicity Δ, where Δ is generally expressed as π/Δ_m.

We now focus on the analysis of third-order combined harmonics at the mixing frequencies $\omega^{(3)} = 2\omega_a \pm \omega_b$ and $\omega_a \pm 2\omega_b$. Thus, we neglect the third-order terms of the self interactions of two primary waves. To analyze the generation of the third-order combined harmonics, the expression for nonlinear terms can, respectively, be simplified as

$$Y^{(3)} = y^{(2a\pm b)}exp\left\{j\left[\left(2k_a \pm k_b\right)z - \left(2\omega_a \pm \omega_b\right)t\right]\right\} +$$

$$+ y^{(a\pm 2b)}exp\left\{j\left[\left(k_a \pm 2k_b\right)z - \left(\omega_a \pm 2\omega_b\right)t\right]\right\},$$

and

$$S^{(3)} \cdot n_x = s^{(2a \pm b)} \cdot n_x expj[(2k_a \pm k_b)z - (2\omega_a \pm \omega_b)t] +$$

$$+ s^{(a \pm 2b)} \cdot n_x exp\left\{ j\left[\left(k_a \pm 2k_b\right)z - \left(\omega_a \pm 2\omega_b\right)t \right]\right\}.$$

Referring to the process of analyzing second-order combined harmonics, the total fields of third-order combined harmonics generated by $y^{(2a \pm b)}, s^{(2a \pm b)} \cdot n_x, y^{(a \pm 2b)}$ and $s^{(a \pm 2b)} \cdot n_x$ can also be written as a linear combination of a series of Lamb waves at the mixing frequencies $\omega^{(3)} = 2\omega_a \pm \omega_b$ and $\omega_a \pm 2\omega_b$

$$v^{(3)} = v^{(2\omega_a \pm \omega_b)} + v^{(\omega_a \pm 2\omega_b)},$$

$$v^{(2\omega_a \pm \omega_b)} = \sum_p \alpha_p \left(z\right) v_p^{(2\omega_a \pm \omega_b)}(x) exp\left[-j(2\omega_a \pm \omega_b)t\right],$$

$$v_p^{(2\omega_a \pm \omega_b)}(x) \; v^{(\omega_a \pm 2\omega_b)} = \sum_q \;_q (z) v_q^{(\omega_a \pm 2\omega_b)}(x) exp\left[-j(\omega_a \pm 2\omega_b)t\right],$$

where $v_p^{(2\omega_a \pm \omega_b)}(x)$ and $v_q^{(\omega_a \pm 2\omega_b)}$ are the field functions of the pth and q^{th} Lamb wave at the mixing frequencies $2\omega_a \pm \omega_b$ and $\omega_a \pm 2\omega_b$, respectively, and $\alpha_p(z)$ and $\beta_q(z)$ the corresponding expansion coefficients.

The analysis of the second-order combined harmonics leads to the equations governing $\alpha_p(z)$ and $\beta_q(z)$ can be given by

$$4Y_{pp}\left[\frac{d}{dz} - jk_p^{(3)}\right]\alpha_p(z) = \left[y_{s,(p)}^{(3)} + y_{b,(p)}^{(3)}\right]exp\left[j\left(2k_a \pm k_b\right)z\right],$$

and

$$4Y_{qq}\left[\frac{d}{dz} - jk_p^{(3)}\right]\alpha_p(z) = \left[y_{s,(p)}^{(3)} + y_{b,(p)}^{(3)}\right]exp\left[j\left(k_a \pm 2k_b\right)z\right],$$

where $k_p^{(3)}$ and $k_p^{(3\beta)}$ are, respectively, the wavenumbers of the Lamb waves at the mixing frequencies $2\omega_a \pm \omega_b$ and $\omega_a \pm 2\omega_b$ and $Y_{pp\alpha}$ and $Y_{qq\beta}$ are the corresponding average power flow per unit width along the ox axis, whose formal expressions are, respectively,

$$Y_{pp\alpha} = Re\frac{1}{2}\int_{-h}^{h}\left[-j\left(2\omega_a \pm \omega_b\right)\right]\begin{bmatrix} n_x v_p^{(2\omega_a \pm \omega_b)}\left(x\right)T_{(p)xz}\left(x\right) \\ n_z v_p^{(2\omega_a \pm \omega_b)}\left(x\right)T_{(p)zz}\left(x\right) \end{bmatrix}dy,$$

$$Y_{qq\beta} = Re\frac{1}{2}\int_{-h}^{h}\left[-j\left(\omega_a \pm 2\omega_b\right)\right]\begin{bmatrix} n_x v_p^{(\omega_a \pm 2\omega_b)}\left(x\right)T_{(q)xz}\left(x\right) \\ n_z v_p^{(\omega_a \pm 2\omega_b)}\left(x\right)T_{(q)zz}\left(x\right) \end{bmatrix}dy,$$

where $T_{(r)xz}(x) = n_x T_r n_z$, $T_{(r)zz}(x) = n_z T_r n_z$, $(r = p, q)$; T_r is the stress tensor related to $v_p^{(2\omega_a \pm \omega_b)}(x)$ or $v_p^{(\omega_a \pm 2\omega_b)}(x)$.

It is important to note that the third-order combined harmonic modes at the mixing frequencies $2\omega_a \pm \omega_b$ and $\omega_a \pm 2\omega_b$ are induced by the third order cross-interaction between the two primary Lamb waves v_a and v_b. Only symmetric second harmonics can be generated by the self-interaction of primary Lamb waves with either asymmetry or antisymmetry feature.

Numerical analysis showed that, the third-order combined harmonic $v^{(2\omega_a \pm \omega_b)}$ at the frequency $2\omega_a \pm \omega_b$ has the same symmetry feature as the primary Lamb wave v_b, while the symmetry feature of $v^{(\omega_a \pm 2\omega_b)}$ at the frequency $\omega_a \pm 2\omega_b$ depends only on that of the primary Lamb wave v_a. Similarly, both the synchronism and symmetry feature should be simultaneously considered for predicting the existence of cumulative third-order combined harmonics generated by the collinear mixing of two primary Lamb waves. The discovered dependencies, both synchronism and symmetry, must be taken into account simultaneously to predict the existence of so-called cumulative combined harmonics of the third order. Such harmonics are generated by collinear mixing of two primary Lamb waves.

4 BASIC RESULTS

Verification of the theoretically discovered dependencies was performed using known experimental studies of the frequency mixing responses of two primary Lamb waves in an aluminum plate with a thickness of $h = 0,97 mm$, a length of $L = 1200\ mm$ along the propagation direction and a width of $h_1 = 480 mm$ perpendicular to the propagation direction.
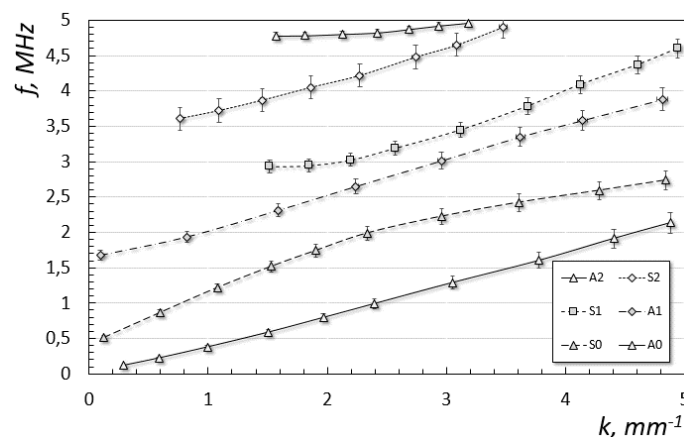

Fig.1. Lamb wave dispersion curves for second-order harmonic mode

At longitudinal and transverse velocities of the plate material (aluminum) set to 6.395 km/s and 3.240 km/s. The dispersion curves of Lamb wave propagation for determining the combined harmonic modes of the second and third order satisfying the synchronism condition are demonstrated in Fig. 1 and 2. In particular, two primary Lamb waves, including the A1 mode at a frequency of f_a = 2.6 MHz and the S0 mode at f_b = 1.35 MHz, are determined for collinear mixing of wave propagation.
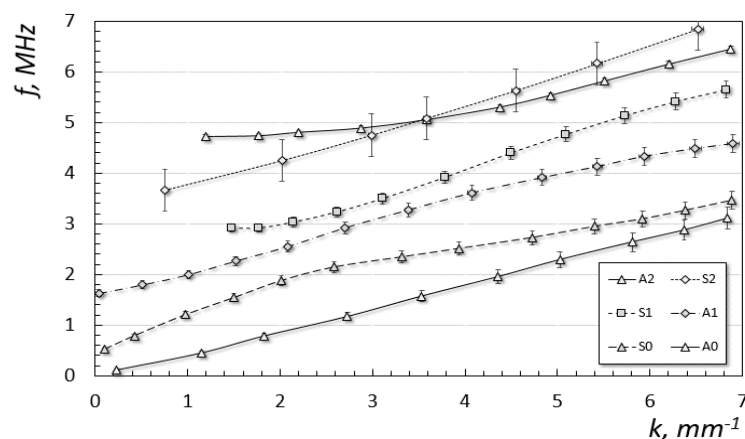

Fig.2. Lamb wave dispersion curves for third-order harmonic mode

The frequencies and phase velocities of the two selected primary Lamb waves, as well as the combined harmonic modes of the second and third orders that satisfy the synchronism condition, can be determined using the dispersion curves of Lamb wave propagation shown in Fig. 3.
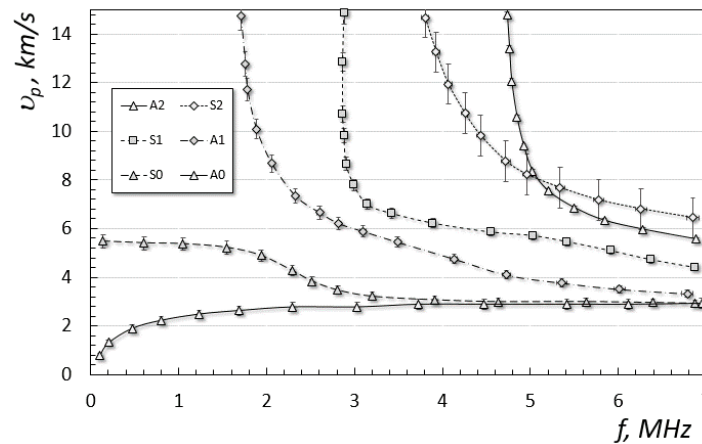

Fig.3. Phase velocity (υ_p) dispersion curves of Lamb waves

5 DISCUSSION OF THE RESULTS OF THE STUDY

The dispersion curves shown in Fig. 1 indicate that the combined second-order harmonic mode (i.e., S1 mode) at the sum frequency of 4.0 MHz satisfies the phase-matching condition (i.e., $k^{(2)} = k_a + k_b$ at $v^{(2)} = v_a + v_b$). On the other hand, it can be argued that there is a clear difference between the wave number of the Lamb wave at $v^{(2)} = v_a - v_b$ and the value $(k_a - k_b)$, which means that the second-order difference frequency mode does not satisfy the phase-matching condition.

The third-order combined harmonic modes satisfying the synchronism condition are shown in Fig. 2. It should be noted that the wave numbers $k_a, k, k^{(2)}$ and $k^{(3)}$ at $v_a, v_b, v_a + v_b$ and $2v_a \pm v_b$ or $(v_a \pm 2v_b)$ depend on the values of the longitudinal and transverse velocities of the plate material.

The results of the calculation methods indicate that the relative error of the calculated values may depend on the longitudinal and transverse velocities of propagation of the Lamb wave modes in the plate material. The reaction of mixing the Lamb waves' frequencies at frequencies $2v_a \pm v_b$ and $v_a \pm 2v_b$ was detected. It can be considered that it approximately satisfies the synchronism criterion for generating third-order combined harmonic modes. Obviously, the third-order combined harmonic modes at the frequency $2v_a \pm v_b$ satisfy the synchronism condition better than at the frequency $v_a \pm 2v_b$.

It can be concluded that for the two selected primary Lamb waves, the synchronism of the generation of combined harmonic modes of the second and third order is considered simultaneously, which means that possible frequency mixing reactions of the second and third orders can be observed simultaneously. The frequency mixing reaction of Lamb waves is indeed manifested for the selected pair of modes.

However, it should be noted that although the combined second-order harmonic mode (i.e., the S1 mode) at the sum frequency satisfies the synchronism condition, the corresponding amplitude is not displayed on the amplitude-frequency curve. The analysis showed that in addition to the synchronism condition, the required symmetry condition must be simultaneously satisfied for the combined second-order harmonic mode to be generated. In particular, the combined second-order harmonic mode generated at the sum frequency

must be antisymmetric rather than symmetric due to the cross-talk between the A1 and S0 modes. Thus, the absence of the appearance of the combined second-order harmonic mode should be explained by the fact that the synchronism and symmetry conditions cannot be simultaneously achieved.

6   CONCLUSIONS

In this paper, the frequency mixing response caused by the collinear cross-talk of two primary Lamb waves with different frequencies is theoretically analyzed and compared with known experimental results. A theoretical basis for the frequency mixing response caused by the collinear mixing of two primary Lamb waves is established using the perturbation approximation and the normal mode decomposition method for waveguide excitation. Based on the theoretical basis, we discuss the internal resonance conditions for the generation of second- and third-order combined harmonics by two primary Lamb waves, and predict the existence of second- and third-order combined harmonics at different mixing frequencies.

To verify the theoretical prediction, the results of the combined harmonics measurements of two primary Lamb waves at certain mixing frequencies are used. The experimental results show that two conditions must be simultaneously satisfied for the combined harmonics to be generated. The first condition is synchronization, and the second condition is the symmetry property. In addition, it can be stated that the frequency mixing response is due only to the collinear cross-talk between the two primary Lamb waves.

In addition, the previously predicted cumulative effect of combined harmonics generated with the propagation distance in the mixing zone of two primary Lamb waves propagating in the sample was found. This effect is consistent with the effect of the appearance of combined harmonics at certain mixing frequencies. Thus, this work provides a physical understanding of the generation of combined harmonic modes by the collinear cross-talk of two primary Lamb waves.

7   ETHICAL DECLARATIONS

The author has no relevant financial or non-financial interests to report.

References

1. Deng, M. Modal analysis of second-harmonic generation of generalized Lamb waves in layered planar structures. Ndt & E International. 2005. 38(2). Pp. 85-95. https://doi.org/10.1016/j.ndteint.2004.05.005
2. Shan, S., & Cheng, L. Mixed third harmonic shear horizontal wave generation: interaction between primary shear horizontal wave and second harmonic Lamb wave. Smart Materials and Structures. 2019. 28(8). P. 085042. https://doi.org/10.1088/1361-665X/ab1fce
3. Yang, Y., Ng, C. T., & Kotousov, A. Second-order harmonic generation of Lamb wave in prestressed plates. Journal of Sound and Vibration. 2019. 460. P. 114903. https://doi.org/10.1016/j.jsv.2019.114903
4. Matsuda, N., & Biwa, S. Frequency dependence of second-harmonic generation in Lamb waves. Journal of Nondestructive Evaluation. 2014. 33. Pp. 169-177. https://doi.org/10.1007/s10921-014-0227-y
5. Xu, C., Yang, Z., Qiao, B., & Chen, X. Sparse estimation of propagation distances in Lamb wave inspection. Measurement Science and Technology. 2019. 30(5). P. 055601. https://doi.org/10.1088/1361-6501/ab04ec
6. Pagneux, V., & Maurel, A. Lamb wave propagation in elastic waveguides with variable thickness. Proceedings of the Royal Society A: Mathematical, Physical and Engineering Sciences. 2006. 462(2068). Pp. 1315-1339. https://doi.org/ 10.1098/rspa.2005.1612

7. Li, W., Deng, M., Hu, N., & Xiang, Y. Theoretical analysis and experimental observation of frequency mixing response of ultrasonic Lamb waves. Journal of Applied Physics. 2018. 124(4). https://doi.org/10.1063/1.5028536

8. Ishii, Y., Biwa, S., & Adachi, T. Non-collinear interaction of guided elastic waves in an isotropic plate. Journal of Sound and Vibration. 2018. 419. Pp. 390-404. https://doi.org/ 10.1016/j.jsv.2018.01.031

9. Novak, A., Bentahar, M., Tournat, V., El Guerjouma, R., & Simon, L. Nonlinear acoustic characterization of micro-damaged materials through higher harmonic resonance analysis. Ndt & E International. 2012. 45(1). Pp. 1-8. https://doi.org/ 10.1016/j.ndteint.2011.09.006

10. Patil, G. U., & Matlack, K. H. Review of exploiting nonlinearity in phononic materials to enable nonlinear wave responses. Acta Mechanica. 2022. 233(1). Pp. 1-46. https://doi.org/ 10.1007/s00707-021-03089-z

11. Liu, M., Tang, G., Jacobs, L. J., & Qu, J. Measuring acoustic nonlinearity parameter using collinear wave mixing. Journal of applied physics. 2012. 112(2). https://doi.org/10.1063/1.4739746

12. Sun, Z., Li, F., & Li, H. A numerical study of non-collinear wave mixing and generated resonant components. Ultrasonics. 2016. 71. Pp. 245-255. https://doi.org/ 10.1016/j.ultras.2016.06.019

13. Tang, G., Liu, M., Jacobs, L. J., & Qu, J. Detecting localized plastic strain by a scanning collinear wave mixing method. Journal of Nondestructive Evaluation. 2014. 33. Pp. 196-204. https://doi.org/ 10.1007/s10921-014-0224-1

14. Jiao, J., Lv, H., He, C., & Wu, B. Fatigue crack evaluation using the non-collinear wave mixing technique. Smart Materials and Structures. 2017. 26(6). P. 065005. https://doi.org/ 10.1088/1361-665X/aa6c43

15. Qiao, R., & Yan, X. The characterization of fatigue damage of 316L stainless steel parts formed by selective laser melting with harmonic generation technique. Materials. 2022. 15(3). P. 718. https://doi.org/ 10.3390/ma15030718

16. Crété, J. P., Longère, P., & Cadou, J. M. Numerical modelling of crack propagation in ductile materials combining the GTN model and X-FEM. Computer Methods in Applied Mechanics and Engineering. 2014. 275. Pp. 204-233. https://doi.org/ 10.1016/j.cma.2014.03.007

17. Zhang, Y., Wang, X., Yang, Q., Xue, R., Zhang, J., Sun, Y., & Krishnaswamy, S. Research on epoxy resin curing monitoring using laser ultrasonic. Measurement. 2020. 158. P. 107737. https://doi.org/ 10.1016/j.measurement.2020.107737

18. Chu, Q., Li, Y., Xiao, J., Huan, D., Zhang, X., & Chen, X. Processing and characterization of the thermoplastic composites manufactured by ultrasonic vibration–assisted automated fiber placement. Journal of Thermoplastic Composite Materials. 2018. 31(3). Pp. 339-358. https://doi.org/ 10.1177/0892705717697781

19. Gao, X., & Qu, J. Necessary and sufficient conditions for resonant mixing of plane waves in elastic solids with quadratic nonlinearity. The Journal of the Acoustical Society of America. 2020. 148(4). Pp. 1934-1946. https://doi.org/10.1121/10.0002009

20. Zhao, Y., Chen, Z., Cao, P., & Qiu, Y. Experiment and FEM study of one-way mixing of elastic waves with quadratic nonlinearity. NDT & E International. 2015. 72. Pp. 33-40. https://doi.org/10.1016/j.ndteint.2015.02.004

Література

1. Deng, M. (2005) Modal analysis of second-harmonic generation of generalized Lamb waves in layered planar structures. *Ndt & E International*. 38(2). 85-95.

2. Shan, S., & Cheng, L. (2019) Mixed third harmonic shear horizontal wave generation: interaction between primary shear horizontal wave and second harmonic Lamb wave. Smart Materials and Structures. 28(8).

3. Yang, Y., Ng, C. T., & Kotousov, A. (2019) Second-order harmonic generation of Lamb wave in prestressed plates. Journal of Sound and Vibration. 2019. 460. P. 114903.

4. Matsuda, N., & Biwa, S. (2014) Frequency dependence of second-harmonic generation in Lamb waves. Journal of Nondestructive Evaluation. 33. 169-177.

5. Xu, C., Yang, Z., Qiao, B., & Chen, X. (2019) Sparse estimation of propagation distances in Lamb wave inspection. Measurement Science and Technology. 30(5). 055601.

6. Pagneux, V., & Maurel, A. (2006) Lamb wave propagation in elastic waveguides with variable thickness. Proceedings of the Royal Society A: Mathematical, Physical and Engineering Sciences. 462(2068). 1315-1339.

7. Li, W., Deng, M., Hu, N., & Xiang, Y. (2018) Theoretical analysis and experimental observation of frequency mixing response of ultrasonic Lamb waves. Journal of Applied Physics. 124(4).

8. Ishii, Y., Biwa, S., & Adachi, T. (2018) Non-collinear interaction of guided elastic waves in an isotropic plate. Journal of Sound and Vibration. 419. 390-404.

9. Novak, A., Bentahar, M., Tournat, V., El Guerjouma, R., & Simon, L. (2012) Nonlinear acoustic characterization of micro-damaged materials through higher harmonic resonance analysis. Ndt & E International. 45(1). 1-8.

10. Patil, G. U., & Matlack, K. H. (2022) Review of exploiting nonlinearity in phononic materials to enable nonlinear wave responses. Acta Mechanica. 233(1). 1-46.

11. Liu, M., Tang, G., Jacobs, L. J., & Qu, J. (2012) Measuring acoustic nonlinearity parameter using collinear wave mixing. Journal of applied physics. 112(2).

12. Sun, Z., Li, F., & Li, H. (2016) A numerical study of non-collinear wave mixing and generated resonant components. Ultrasonics. 71. 245-255.

13. Tang, G., Liu, M., Jacobs, L. J., & Qu, J. (2014) Detecting localized plastic strain by a scanning collinear wave mixing method. Journal of Nondestructive Evaluation. 33. 196-204.

14. Jiao, J., Lv, H., He, C., & Wu, B. (2017) Fatigue crack evaluation using the non-collinear wave mixing technique. Smart Materials and Structures. 26(6). 065005.

15. Qiao, R., & Yan, X. (2022) The characterization of fatigue damage of 316L stainless steel parts formed by selective laser melting with harmonic generation technique. Materials. 15(3). 718.

16. Crété, J. P., Longère, P., & Cadou, J. M. (2014) Numerical modelling of crack propagation in ductile materials combining the GTN model and X-FEM. Computer Methods in Applied Mechanics and Engineering. 275. 204-233.

17. Zhang, Y., Wang, X., Yang, Q., Xue, R., Zhang, J., Sun, Y., & Krishnaswamy, S. (2020) Research on epoxy resin curing monitoring using laser ultrasonic. Measurement. 158. 107737.

18. Chu, Q., Li, Y., Xiao, J., Huan, D., Zhang, X., & Chen, X. (2018) Processing and characterization of the thermoplastic composites manufactured by ultrasonic vibration–assisted automated fiber placement. Journal of Thermoplastic Composite Materials. 31(3). 339-358.

19. Gao, X., & Qu, J. (2020) Necessary and sufficient conditions for resonant mixing of plane waves in elastic solids with quadratic nonlinearity. The Journal of the Acoustical Society of America. 148(4). 1934-1946.

20. Zhao, Y., Chen, Z., Cao, P., & Qiu, Y. (2015) Experiment and FEM study of one-way mixing of elastic waves with quadratic nonlinearity. NDT & E International. 72. 33-40

Alexander Pysarenko
Odesa State Academy of Civil Engineering and Architecture
Ph.D., Associate Professor
Didrihsona str., 4, Odesa, Ukraine, 65029
pysarenkoan@gmail.com,
ORCID: 0000-0001-5938-4107